THREE-DIMENSIONAL SOUND FIELD REPRODUCTION AND RECORDING SYSTEMS BASED ON BOUNDARY SURFACE CONTROL PRINCIPLE

Seigo Enomoto†, Yusuke Ikeda†, Shiro Ise‡ and Satoshi Nakamura†

† Advanced Telecommunication Research Institute International,
Spoken Language Communication Research Laboratories,
2-2-2 Hikaridai , Keihanna Science City, Kyoto, 619–0288 Japan
{seigo.enomoto, yusuke.ikeda, satoshi.nakamura}@atr.jp

‡ Urban and Environmental Engineering, Graduate School of Engineering, Kyoto University,
C1–386, Kyodai-Katsura, Nisikyo-ku, Kyoto-shi, 615–8540 Japan
ise@archi.kyoto-u.ac.jp

ABSTRACT

Based on the boundary surface control (BSC) principle, a new recording/reproduction system is developed to realize high fidelity three-dimensional sound field reproduction. Theoretically, using this new system, perfect sound field reproduction can be achieved in any acoustic environment. Sound recording / reproduction systems based on the BSC principle require many loudspeakers and microphones. In the new system, the microphone array system that is used to record the 3D sound field consists of 70 microphones, and the loudspeaker system to reproduce the recorded 3D sound field consists of 62 full-range units and eight sub-woofer units.

This paper describes the composition of the new recording/ reproduction system and evaluates its ability by means of sound localization tests with nine subjects. Results of experiments show that a clear sound image in the horizontal plane is reconstructed using the proposed system.

1. INTRODUCTION

Due to the improved performance of computer hardware and the increased speed of Internet access, practical applications of telecommunication systems that transmit visual, auditory, haptic, and aromatic information are expected in the near future. The ultimate goal of such technologies is for people in distant places to communicate with each other as if they were in the same place. Humans recognize their environment (including other people) through the five senses and their integration. Telecommunication systems, however, assume that visual and auditory perception are more important than the other senses. Moreover, auditory information is perceived from all directions surrounding the listener. In contrast, visual information is only perceived from sight. Hence, in telecommunication systems in which many people participate at the same time, auditory perception is more important than visual perception. To create a highly realistic massive 3D sound field, various auditory displays and sound reproduction systems have been invented [1][2][3]. Auditory displays and sound reproduction systems can be classified into two types based on the following questions. First, are users required to wear a device? Second, can a perfect, original sound field theoretically be recorded/reproduced?

In a binaural system, which is one system that requires the user to wear a device, the user wears a headset. Binaural signals are generally recorded by a Head and Torso Simulator (HATS) and then reproduced at the user's ears. Various directions and distances can be presented to users with such systems because the head-related transfer functions (HRTFs) of HATS are included in the binaural signals. HRTF databases, which are usually measured in an anechoic chamber, are published [4][5]. A binaural system is widely used for analyzing and designing industrial sound, since the scale of the system is very small and perfect sound signals can

Figure 1: C80 fullerene structure microphone array to record a 3D sound field with seventy nodes having intervals of around eight cm. 70 omni-directional microphones are installed on each node position.

Figure 2: Loudspeaker system to reconstruct a 3D sound field recorded by a C80 fullerene-structured microphone array that consists of a dome structure and a support pillar. The dome structure part has four mounting racks and six full-range units, and 16, 24, and 16 units are installed on them, respectively.

Figure 3: 3D sound field reproduction room. This room is constructed using a sound-proofed room to reduce the noise. The loudspeaker system, a hydraulic lift and a chair are installed in the room. The hydraulic lift and the chair raise the user's head into the 3D sound field reproduced area.

be reconstructed. The sound signal, however, is reproduced only at the user's ears. This means that spatial sound reproduction cannot be achieved. Thus, it is difficult to follow user movements or head rotation. Binaural systems, that can follow the rotation of the user's head, have also been developed[6][7]. Using this system, perfect sound reproduction can be achieved because the appearance of HATS is quite familiar to users. On the other hand, when the appearance of HATS is different from users, it is difficult to achieve correct sound localization. Note that if HATS can rotate its head simulator to obey the user, the user can correctly find the sound image, even when the appearance is not familiar. HRTFs can also be obtained by computational calculations[8][9]. This research field has become very attractive in recent years. In a free sound field, the HRTFs of all sound source positions can be calculated in several hundred milliseconds [10]. However, reconstructing perfect sound fields is impossible because the calculation of HRTFs requires huge computational complexity since all boundary conditions must be solved in practical situations.

On the other hand, various spatial sound reproduction systems using loudspeakers have been invented that generally don't require users to wear a device. Stereophony is one such a system. Other types include a trans-aural system [11] and wave field synthesis (WFS) [12]. Traditional stereophony uses two or more loudspeakers and typically operates with five-channel surround loudspeakers and a one-channel sub-woofer. These systems are already widely used in home and movie theaters. However, they have no theoretical background upon which to reconstruct a perfect sound field because their spatial audio sound is usually created by musicians or editors. In trans-aural systems, a pair of loudspeakers are used to reconstruct the binaural signals at the user's ears. Usually, binaural signals are recorded using HATS or obtained from numerical calculations. Perfect original sound signals can be reconstructed using this system. However, user movement and rotation are not supported because spatial sound reproduction is not realized. Based on Huygens' principle, WFS is a 3D stereophony system in which a perfect 3D sound field can be theoretically recorded and reconstructed. However, it requires an anechoic chamber as a reproduction room, due to the theoretical constraints of Huygens' principle. Therefore, performance in real environments might be lowered by reflections from walls and so on[13].

In this paper, a new 3D sound field recording and reproduction system based on the boundary surface control principle (BSC) [14] is proposed. In this new system, users don't have to wear a device. Furthermore, a perfect sound field can be reconstructed without any constraints or compensation.

2. SOUND FIELD REPRODUCTION SYSTEM

Our proposed sound field recording and reproduction system based on the BSC principle consists of three parts. The first is a microphone array for recording a perfect 3D sound field. The second is a loudspeaker system to reproduce the perfect 3D sound field

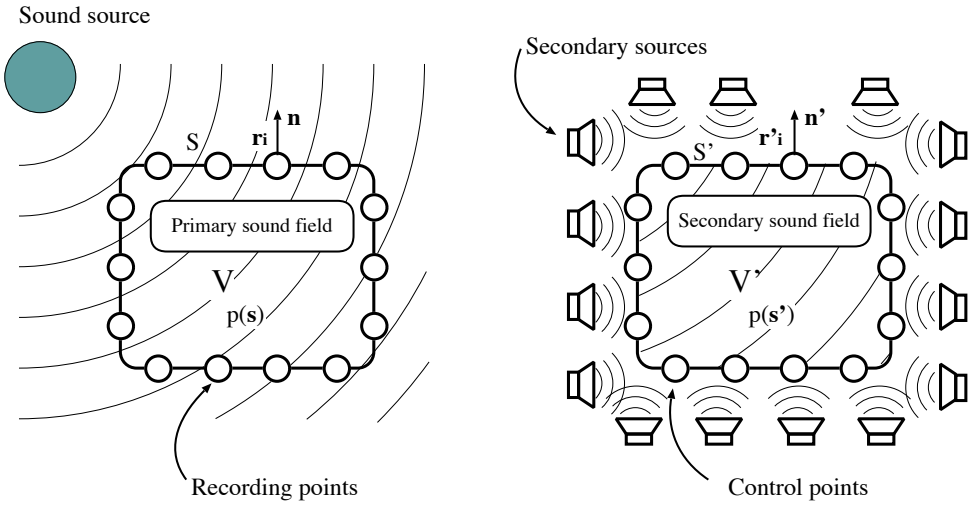

Figure 4: A 3D sound field reproduction system based on the BSC principle. The left picture shows the primary sound field. The right picture shows the secondary sound field. Based on the BSC principle, the sound field enclosed by virtual surface $\mathbf{S}'$ in the secondary sound field is completely equal to the sound field enclosed by $\mathbf{S}$ in the primary sound field.

recorded by the microphone array. The third is a 3D sound reproduction room for use as a listening room in which the sound field is reconstructed. The construction of these three parts of the proposed system is described in this section.

2.1. C80 fullerene structure microphone array to record 3D sound field

A 3D sound recording system that is based on the BSC principle requires a microphone array that can enclose any 3D sound field to be reproduced. In the new recording system, the microphone array has 70 elements that consist of parts of the C80 fullerene structure [15]. This microphone array geometry was selected because of its robustness and easy assembly. Figure 1 shows the proposed microphone array. Seventy omni-directional microphones (DPA 4060-BM), installed on each node position, are connected to an Analog-to-Digital Converter (ADC) through a pre-amplifier, and the sound signals are recorded in synchronization with a 48 kHz sampling frequency.

2.2. Loudspeaker system to reproduce 3D sound field recorded by C80 microphone array

The loudspeaker system is comprised of an oval dome structure that is supported by four pillars.

The oval dome structure consists of four racks, and full-range loudspeaker units (FOSTEX FE83E) are installed on each rack. The top rack has six speaker units, the upper-middle rack has sixteen, the lower-middle rack has twenty-four, and the lower rack has sixteen. Furthermore, each pillar has two sub-woofer units (FOSTEX FW108N) to supply lower frequency responses. The four oval domes and pillars have a cavity as an enclosure for the loudspeaker units. The proposed loudspeaker systems are shown in Figure 2. The height of the lower-middle rack, in which 24 full-range speaker units are installed, supposedly equals the height of the user's ears.

2.3. 3D sound field reproduction room

The 3D sound field reproduction room is constructed using a soundproofed room 1,375 mm $\times$ 1,818 mm $\times$ 2,256 mm with a sound insulation rating of D_r30. Figure 3 shows the 3D sound reproduction room. The loudspeaker system described in the previous section, a hydraulic lift, and a chair are installed in this room. The hydraulic lift raises the user's head into the 3D sound field reproduced area.

3. THEORY

3.1. Sound reproduction system based on BSC principle

The boundary surface control principle combines a wave equation theory with a multiple-input/multiple-output system and proves that the sound field enclosed by the virtual surface can be controlled by sound pressure and particle velocity [14]. A general illustration of the sound field reproduction based on the BSC principle is represented in Figure 4. The goal of BSC-based sound field reproduction is to reproduce sound field V enclosed by surface S into V' in the secondary sound field. Note that the arrangement of *recording points* $\mathrm{r_i}$ on surface S should equal *control points* $\mathrm{r_i'}$ on S'. That is, the relationship between arbitrary point $\mathbf{s}$ in fields V and $\mathbf{r}$ is defined as:

$$|\mathbf{r}-\mathbf{s}| = |\mathbf{r}'-\mathbf{s}'|, \forall \mathbf{r}, \mathbf{s} \in V, \forall \mathbf{r}', \mathbf{s}' \in V'. \quad (1)$$

When Eq. (1) can be assumed, sound pressures $p(\mathbf{s})$ and $p(\mathbf{s}')$ inside V and V' respectively are expressed as:

$$p(\mathbf{s}) = \int_S \left\{ \frac{\partial p(\mathbf{r}|\mathbf{s})}{\partial n} G(\mathbf{r}|\mathbf{s}) - p(\mathbf{r}) \frac{\partial G(\mathbf{r}|\mathbf{s})}{\partial n} \right\} dS, \quad (2)$$

and

$$p(\mathbf{s}') = \int_{S'} \left\{ \frac{\partial p(\mathbf{r}'|\mathbf{s}')}{\partial n'} G(\mathbf{r}'|\mathbf{s}') - p(\mathbf{r}') \frac{\partial G(\mathbf{r}'|\mathbf{s}')}{\partial n'} \right\} dS', \quad (3)$$

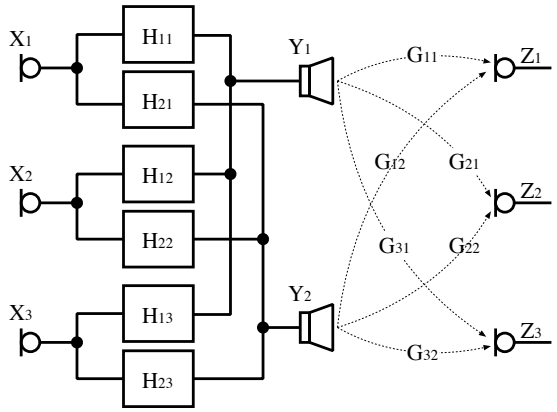

Figure 5: Block diagram form of sound recording/reproduction systems. X, Y, and Z are the recorded audio, radiation, and desired signals, respectively. In this figure, $M = 2$ and $N = 3$ are supposed. When $X = Z$, a perfect sound field is reconstructed.

using the Kirchhoff-Helmholtz boundary integral equation. Here ω is the frequency, and ρ_0 is the medium density. $p(\mathbf{r})$ and $\frac{\partial p(\mathbf{r}|\mathbf{s})}{\partial n}$ are the sound pressure and its gradient at $\mathbf{r}$ on the surface. If we can assume Eq. (1), then the relationship between Greens' function $G(\mathbf{r}|\mathbf{s})$ and its gradient in the primary and secondary field can be written as

$$G(\mathbf{r}|\mathbf{s}) = G(\mathbf{r}'|\mathbf{s}') \quad (4)$$

$$\frac{\partial G(\mathbf{r}|\mathbf{s})}{\partial n} = \frac{\partial G(\mathbf{r}'|\mathbf{s}')}{\partial n'}. \quad (5)$$

Therefore, when the sound pressure and its gradient represented in Eqs. (2) and (3) can be written as:

$$\begin{cases} p(\mathbf{r}) = p(\mathbf{r}'), \\ \dfrac{\partial p(\mathbf{r}|\mathbf{s})}{\partial n} = \dfrac{\partial p(\mathbf{r}'|\mathbf{s}')}{\partial n'} \end{cases} (\forall \mathbf{r} \in S, \forall \mathbf{r}' \in S'), \quad (6)$$

it is verified that

$$p(\mathbf{s}) = p(\mathbf{s}') \ (\forall \mathbf{s} \in V, \forall \mathbf{s}' \in V'). \quad (7)$$

Equations (6) and (7) mean that the sound pressure and its gradient recorded on surface *S* equal those on *S'*, and the sound field inside *V* can be reproduced in *V'*. The gradient of the sound pressure on the surface can be expressed as the difference of the sound pressure measured at both points that cross the surface. However, in the proposed sound field reproduction system, the sound field is controlled by the sound pressure measured by the microphone located on the surface in the primary and secondary fields to reduce system complexity. This is because the sound field enclosed by the surface can be controlled either by the sound pressure or by its gradient except for the natural frequency defined by surface *S*[16].

3.2. Inverse filter design method in frequency domain

To reproduce the sound signals measured on the surface in the primary sound field onto the secondary field, inverse filters are required to cancel the spacial crosstalk between all secondary sources and the control points represented in Figure 5.

The authors previously realized a sound reproduction system that enables the reproduction of a sound field around user's head as a prototype system. In this prototype system, the secondary sources are arranged very close to the control points; that is, the secondary sources and the control points have an identical structure. It is assumed that crosstalk between the secondary sources and the control points can be ignored [17]. Hence, the inverse filters only have characteristics to cancel the transfer function between a corresponding sound source and a control point. However, the arrangement of the secondary sources (Figure 2) in this new sound field reproduction system is different from the structure of the control points. Moreover, crosstalk must be considered because the intervals between the secondary sources and the control points are not close enough to ignore.

The number of secondary sources and control points is specified by *M* and *N*, respectively. The transfer functions between secondary source *i* and control point *j* are specified by $G_{ji}(\omega)$ in the frequency domain. When the sound signal recorded in the primary field is $X_j(\omega)$, the sound signal emitted from the secondary sources is $Y_i(\omega)$, the sound signal measured at the control points is $Z_j(\omega)$, and the input / output relationship of this sound field reproduction system is defined by the following equation:

$$\begin{aligned} \mathbf{Z}(\omega) &= [\mathbf{G}(\omega)]\mathbf{Y}(\omega) \\ &= [\mathbf{G}(\omega)][\mathbf{H}(\omega)]\mathbf{X}(\omega), \end{aligned} \quad (8)$$

where

$$\begin{aligned} \mathbf{X}(\omega) &= [X_1(\omega), \cdots, X_N(\omega)]^T, \\ \mathbf{Y}(\omega) &= [Y_1(\omega), \cdots, Y_M(\omega)]^T, \\ \mathbf{Z}(\omega) &= [Z_1(\omega), \cdots, Z_N(\omega)]^T, \\ [\mathbf{G}(\omega)] &= \begin{bmatrix} G_{11}(\omega) & \cdots & G_{1M}(\omega) \\ \vdots & \ddots & \vdots \\ G_{N1}(\omega) & \cdots & G_{NM}(\omega) \end{bmatrix} \ and \\ [\mathbf{H}(\omega)] &= \begin{bmatrix} H_{11}(\omega) & \cdots & H_{1N}(\omega) \\ \vdots & \ddots & \vdots \\ H_{M1}(\omega) & \cdots & H_{MN}(\omega) \end{bmatrix}. \end{aligned}$$

Since the object in the sound field reproduction system is to achieve $\mathbf{Z}(\omega) = \mathbf{X}(\omega)$, $[\mathbf{H}(\omega)]$ is derived by the inverse matrix of transfer function matrix $[\mathbf{G}(\omega)]$. That is, estimated inverse filter $[\widehat{\mathbf{H}}(\omega)]$ can be derived from the following equation [18][19]:

$$[\widehat{\mathbf{H}}(\omega)] = ([\mathbf{G}(\omega)]^\dagger[\mathbf{G}(\omega)] + \beta\mathbf{I}_M)^{-1}[\mathbf{G}(\omega)]^\dagger. \quad (9)$$

Here, † shows the complex conjugation of the matrix, β is the regularization parameter, and $\mathbf{I}_M$ is an $[M \times M]$ identity matrix. If the number M of loudspeakers which is less than the number N of control points, then the inverse filters are calculated as the least squares problem and when $M = N$, the inverse filters are calculated as the regular inverse matrix. Moreover, in the case of $M > N$, the inverse filters are calculated as the minimum norm solution.

4. SOUND LOCALIZATION TEST

To evaluate the ability of this system, we conducted a sound localization test.

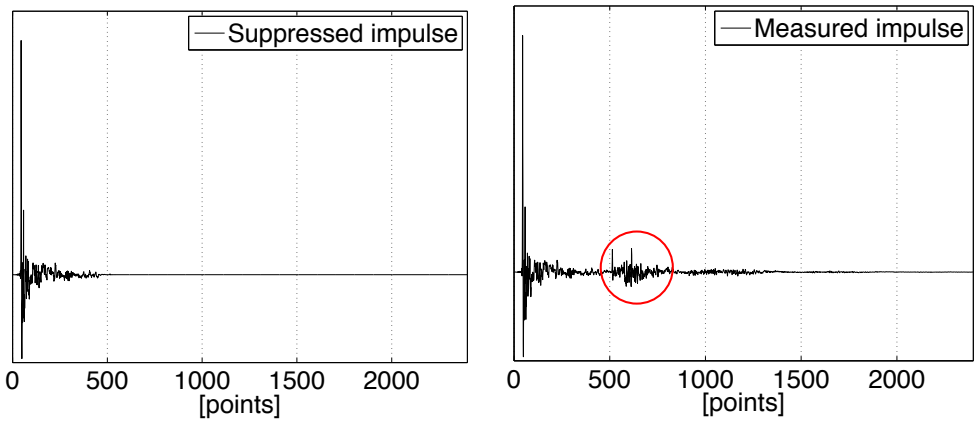

(a) with suppression (b) without suppression

Figure 6: Impulse response measured in the sound field reproduction system.

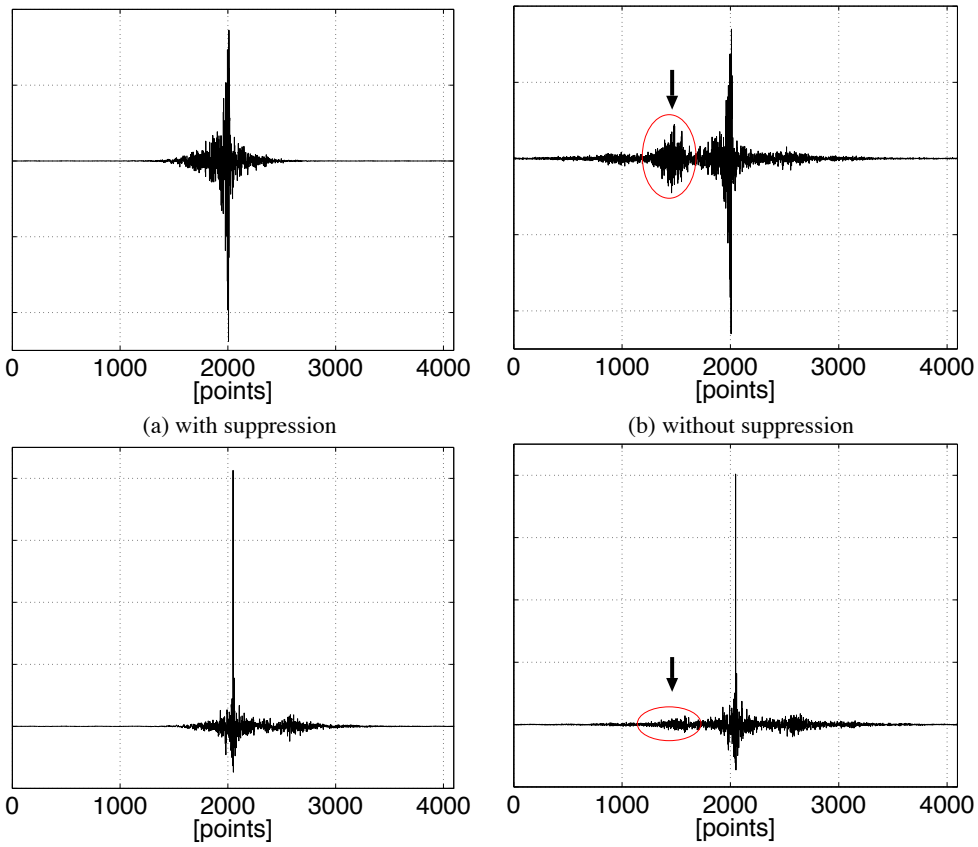

(a) with suppression (b) without suppression

(c) with suppression (d) without suppression

Figure 7: Example of filter coefficient and waveform of response on control points: (a) and (b) show the coefficients of loudspeaker radiation signals. (c) and (d) show the waveform of response on a certain control point.

4.1. Inverse filter calculation

To obtain the inverse filters, the C80 microphone array was set inside the loudspeaker system to measure the impulse responses between the secondary sound source and the control points. The loudspeaker system described above has 62 full-range and eight sub-woofer units. In this experiment, however, since the full-range units installed on the dome structure are used for the secondary sources, we used 62. Each impulse response, which has coeffi-

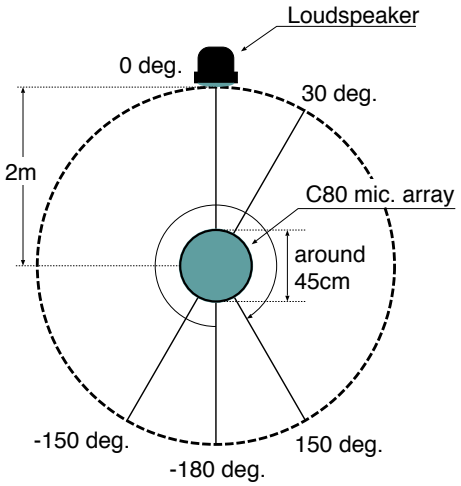

Figure 8: Illustration of experimental setup. Impulse responses are measured on a circle with a 2.0 m radius with an interval angle of 30^o

Figure 9: Experimental setup. Impulse responses between sound source and C80 microphone array are measured in an anechoic room.

cients of 2,400 points length, is measured by the swept-sine signal of 2^{18} points[20] with a 48 kHz sampling frequency and a 24 quantization bit number. The higher frequency range in the sound field reproduction system is limited by approximately 2 kHz, because the intervals between the microphones installed on the C80 microphone array are approximately eight cm. However, to preserve the high-definition audio signals, the inverse filters are calculated in a frequency range above 160 Hz to 24 kHz. Note that reverberation, apparently separated from the direct sound, is eliminated in the impulse responses. The impulse response measured in the sound field reproduction system is depicted in Figs. 6(a) and (b). Figure 6(a) is the impulse response in which reverberation after 500 points is suppressed, and (b) is the original impulse response. The inverse filters are calculated using the impulse response without reverberation; reverberation, which apparently occurred in the sound reproduction room, cannot be suppressed. Perfect sound reproduction cannot be achieved. Consequently, to evaluate the accuracy of the sound signal reproduction at the control points, the spectrum distortion (SD) is calculated in a frequency range above 160Hz to 2kHz on certain control points by a simulated experiment. SD can be written as:

$$\mathrm{SD[dB]} = \sqrt{\frac{1}{K}\sum_{\omega}^{K}\left(20\log|Z_j(\omega)| - 20\log|\widehat{Z_j}(\omega)|^2\right)}, \quad (10)$$

where K is the number of frequencies, and $Z_j(\omega)$ and $\widehat{Z_j}(\omega)$ are the desired and reproduced signals on certain control points. In this experiment, impulse responses measured in the sound field reproduction room are used. The result of this simulated experiment shows that SD in which the reverberation is not suppressed is approximately 5.79 dB, and when the reverberation is suppressed, it is approximately 6.16 dB. Hence, the accuracy of the reproduction signals at the control points is almost identical. On the other hand, to calculate the inverse filter using the impulse response in which the reverberation is not suppressed, large coefficients occurred before the center of the inverse filter in the waveform, as depicted in Fig. 7(b). Echo signals might be generated due to these large coefficients in the reproduced sound signals. Moreover, very small noise appears in the wave domain response on the control point, as depicted in Fig. 7(d). Consequently, in this experiment, impulse responses with reverberation suppression are used to calculate the inverse filter. In this experiment, the inverse filters of 4096 points are calculated in the frequency domain, and $\beta = 6.5 \times 10^{-2}$.

4.2. Making stimuli

A stimulus is made by the convolution of the impulse response measured on a circle with a 2.0 m radius with an interval angle of 30^o in an anechoic room and pink noise. The experimental setup is depicted in Figs. 8 and 9.

4.3. Experimental procedure

Stimuli were generated in the sound field reproduction system. Subjects were four males and five females with normal hearing whose ages ranged from early 20s to late 40s. They were allowed to move their head and body during this experiment. The duration of the source signal mentioned in the previous section was 4 sec with a 1-sec interval for certain directions. A 4-sec interval exists between one direction and another. Subjects were asked to indicate the perceived direction of the presented sound on answer sheets. During these experiments, the room light was on, and so the loudspeaker arrangement could be observed by the subjects. Furthermore, the sound signals in each direction were presented to the subjects one at a time.

4.4. Experimental results

The presented and perceived directions in the horizontal plane of the subject ear heights were compared. Experimental results are shown in Fig. 10. The vertical and horizontal axes show the perceived direction and the source signal presented direction, respectively. The radius of the circle expressed the number of subject answers; that is, the large circle represented the largest number of answers. Almost all subjects perceived the direction of the sound image in the same direction as presented. To investigate the accuracy of the subjective tests, the root mean square (RMS) of the

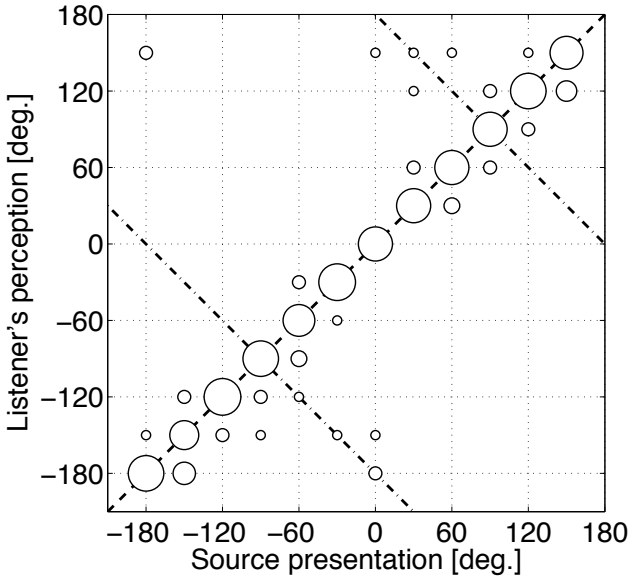

Figure 10: Relation of presented direction to perceived direction in horizontal plane including subject ear height.

difference was averaged between the perceived and presented directions. Averaged RMS is defined by the following equation:

$$\overline{RMS}[\text{deg.}] \quad = \quad \frac{1}{K_j}\sum_j \sqrt{\frac{1}{K_i}\sum_i \left|L_j - \widetilde{L}_{i,j}\right|^2}. \quad (11)$$

Here, L_i and $\widetilde{L}_{i,j}$ are the presented direction of the sound source and the perceived direction, respectively. $i(= 1, \cdots, K_i)$ is the total number of subject answers. $j(= 1, \cdots, K_j)$ is the number of presented directions. In this experiment, $\overline{RMS}$ is achieved as 23.7^o. In contrast, the prototype system achieved 37.0^o in identical experimental conditions. Hence, the performance of the sound source localization test improved approximately 13^o more than the prototype system [17].

5. DISCUSSION

The authors are currently trying to apply the sound field reproduction system based on the BSC principle to *the Sound Field Sharing* (SFS) system[21]. The sound field sharing system enables the user to converse with each other as if they were sharing the same massive sound field. The block diagram form of the sound field sharing system is depicted in Figure 11. The SFS system consists of two or more sound field reproduction systems described in this paper. $\mathbf{H_1}$ and $\mathbf{H_2}$ are the inverse filters that are derived from the transfer functions measured in the sound field reproduction room. $\mathbf{N_1}$ and $\mathbf{N_2}$ are the ambient sound recorded in the sound field database. $\mathbf{L_{12}}$ and $\mathbf{L_{21}}$ are the transfer functions between the user as speaker and the listener in the shared sound field, and $\mathbf{L_{11}}$ and $\mathbf{L_{22}}$ are the transfer functions for the feed-back canceller.

6. CONCLUSION

Based on the BSC principle, a sound field reproduction system comprised of a loudspeaker system, a microphone array, and a sound field reproduction room was described. Moreover, the ability of this system was evaluated by nine subjects who tested the sound source localization. Experimental results showed that the represented ability of the new system is approximately 13^o better than a prototype system previously developed by the authors.

Furthermore, a sound field sharing system is also introduced in this paper. By using the sound field sharing system, a user can converse with other users as if they were in the same sound field.

7. ACKNOWLEDGMENTS

Part of this study was supported by the Strategic Information and Communications R&D Promotion Program commissioned by the Ministry of Internal Affairs and Communications of Japan, and Special Coordination Funds for Promoting Science and Technology of the Ministry of Education, Culture, Sports, Science and Technology of Japan.

8. REFERENCES

[1] Jens Blauert. *Spatial Hearing: the psychophysics of human sound localization - revised edition*. The MIT Press, London, England, 1997.

[2] John Garas. *Adaptive 3D Sound Systems*. Kluwer Academic Publisher, 2000.

[3] Shouichi Takane, Yoiti Suzuki, Tohru Miyajima, and Toshio Sone. A new theory for high definition virtual acoustic display named advise. *Acoustical Science and Technology*, Vol. 24, No. 5, pp. 276–283, 2003.

[4] William G. Gardner and Keith D. Martin. Hrtf measurements of a kemar. *Journal of Acoustical Society of America*, Vol. 97, No. 6, pp. 3907–3908, June 1995.

[5] V. R. Algazi, R. O. Duda, and D. M. Thompson. The cipic hrts database. In *Proc. 2001 IEEE Workshop on Applications of Signal Processing to Audio and Electroacoustics*, pp. 99–102, NY, USA, Oct. 2001.

[6] I. Toshima, H. Uematsu, and T. Hirahara. A steerable dummy head that tracks three-dimensional head move-ment: *Tele Head. Acoust. Sci. & Tech.*, Vol. 24, pp. 327–329, 2003.

[7] Iwaki Toshima and Shigeaki Aoki. Effect of driving delay with an acoustical tele-presence robot, telehead. In *Proceedings of the 2005 IEEE International Conference on Robotics and Automation*, 2005.

[8] Brian F.G. Katz. Boundary element method calculation of individual head-related transfer function. i. rigid model calculation. *Journal of Acoustical Society of America*, Vol. 110, No. 5, pp. 2440–2448, Nov. 2001.

[9] Tian Xiao and Qing Huo Liu. Finite difference computation of head-related transfer function for human hearing. *Journal of Acoustical Society of America*, Vol. 113, No. 5, pp. 2434–2441, May 2003.

[10] Makoto Otani and Shiro Ise. A fast calculation method of the head-related transfer function based on boundary element method. *Journal of Acoustical Society of America*, Vol. 119, pp. 2589–2598, 2006.

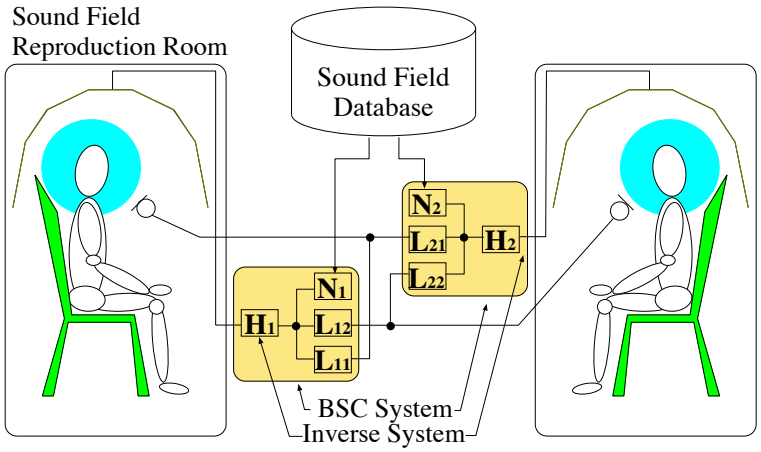

Figure 11: Block diagram form of the sound field sharing (SFS) system. The SFS system consists of two or more sound field reproduction system. The SFS system users can converse with each other as if they were sharing the same sound field.

[11] M. R. Schroeder and B. S. Atal. Computer simulation of sound transmission in rooms. *IEEE Int. Conv. Rec.*, Vol. 7, pp. 150–155, 1963.

[12] A. J. Berkhout, D. de Vries, and P. Vogel. Acoustic control by wave field synthesis. *Journal of Acoustical Society of America*, Vol. 93, pp. 2764–2778, 1993.

[13] Sascha Spors, Herbert Buchner, Rudolf Rabenstein, and Wolfgang Herbordt. Active listening room compensation for massive multichannel sound reproduction systems using wave-domain adaptive filtering. *Journal of Acoustical Society of America*, Vol. 122, No. 1, pp. 354–369, July 2007.

[14] Shiro Ise. A principle of sound field control based on the kirchhoff-helmholtz integral equation and the theory of inverse systems. *Acoustica*, Vol. 85, pp. 78–87, 1999.

[15] P. W. Fowler and D. E. Manolopoulos. *An Atlas of FULLERENES*. Dover Publications, 2007.

[16] R. Kleinman and G. Roach. Boundary integral equations for the three dimensional helmholtz equation. *SIAM Review*, Vol. 16, pp. 214–236, 1974.

[17] Kosuke Okada, Takayuki Kawaguchi, Seigo Enomoto, and Shiro Ise. A develepment of a compact immersive auditory display device and its evaluation. *Journal of Acoustical Society of Japan*, Vol. 62, No. 1, pp. 32–41, 2006. (in Japanese).

[18] Gene H. Golub and Charles F. Van Loan. *Matrix computations*. The Johns Hopkins University Press, 1996.

[19] Hironori TOKUNO, Ole KIRKEBY, Philip A. NELSON, and Hareo HAMADA. Inverse filter of sound reproduction systems using regularization. *IEICE TRANSACTIONS on Fundamentals of Electronics, Communications and Computer*, Vol. E80-A, No. 5, pp. 809–820, 1997.

[20] Yoiti Suzuki, Futoshi Asano, Hack-Yoon Kim, and Toshio Sone. An optimum computer-generated pulse signal suitable for the measurement of very long impulse responses. *Journal of the Acoustical Society of America*, Vol. 97, No. 2, pp. 1119–1123, 1995.

[21] Name of Author. The development of the sound field sharing system based on the boundary surface control principle. In *Proceeding of 19th International Congress on Acoustics*, 2007.